Acta Cryst. (1984). B40, 355–359

An Electron Microscope Examination of Scandium Sesquisulphide, Sc_2S_3, and Its Mode of Disordering in the Electron Beam

BY L. C. OTERO-DIAZ,* K. HIRAGA,† J. R. SELLAR AND B. G. HYDE

Research School of Chemistry, Australian National University, GPO Box 4, Canberra, ACT 2601, Australia

(*Received* 20 *October* 1983; *accepted* 5 *March* 1984)

Abstract

[1$\bar{1}$0] zone-axis structure images of the semiconductor compound Sc_2S_3 show the ordered arrangement of the unoccupied cation positions, which gives rise to a superlattice of the NaCl ($B1$, ScS) structure in three dimensions. The experimental images are adequately simulated by multislice computations. Electron-beam irradiation damages the crystal and the image changes in a complex way. Significant structural changes were directly observed in lattice images and diffraction patterns. Some of this resembles the disorder, believed to be grown in, which consists of antiphase boundaries resulting from the systematic displacement of slabs of structure. [For single crystal: a = 10·376 (2), b = 7·3775 (9), c = 22·033 (6) Å.]

Introduction

There is ample chemical evidence to justify the inclusion of Sc (and Y) with the lanthanoid elements. Although together these form a homogeneous group, there are five different crystal structures reported for their sesquichalcogenides, M_2X_3 (M = 'rare-earth' cation, X = S, Se, Te) (Picon, Domange, Flahaut, Guitard & Patrie, 1960; Flahaut & Laruelle, 1968; Flahaut, 1979). In this group Sc has the shortest bond length to S, and Sc_2S_3 is one of the structure types. Its study commenced over fifty years ago when it was prepared by the action of H_2S on $ScCl_3$ (Klemm, Meisel & von Vogel, 1930). Attempts then made to deduce its structure from X-ray powder diffraction analysis were unsuccessful. Much later, similar studies (Men'kov, Komisatova, Simanov & Spitsyn, 1961*a*,*b*, 1962) led to the conclusion that it was isostructural with β-In_2S_3 (Rooymans, 1959): tetragonal, with a = 10·37 (1), c = 31·11 (3) Å. Finally, Dismukes & White (1964) solved the structure by single-crystal X-ray diffraction, and found it to be orthorhombic, space group *Fddd*, with a = 10·41 (1), b = 7·38 (1), c = 22·05 (2) Å.

Their description is as a superstructure of the **NaCl** ($B1$) type of ScS (which has a = 5·19 Å), with a complex, ordered arrangement of vacant cation sites. The unit cell of Sc_2S_3 (Z = 16; subscript 1) is related to the $B1$ subcell (subscript 0) in the following way:

$\mathbf{a}_1 = 2\mathbf{a}_0$ so that a_1 = 10·41 (1) Å = $2a_0 = 2\times5\cdot2_1$ Å;

$\mathbf{b}_1 = \mathbf{b}_0 - \mathbf{c}_0$ so that b_1 = 7·38 (1) Å = $\sqrt{2}a_0 = \sqrt{2}\times5\cdot2_2$ Å;

$\mathbf{c}_1 = 3(\mathbf{b}_0 + \mathbf{c}_0)$ so that c_1 = 22·05 (2) Å = $3\sqrt{2}a_0 = 3\sqrt{2}\times5\cdot2_0$ Å.

All the atom coordinates are surprisingly close to those for the idealized structure, which is shown in Fig. 1.

This structure, the so-called δ form of M_2S_3, is also that adopted by various rare-earth selenides and tellurides (Dismukes & White, 1965; Flahaut & Laruelle, 1968) and, recently, the same unit cell has been reported for the structure of Lu_3S_4: a = 10·747(3), b = 22·813(6), c = 7·602(2) Å. However, in this case, the occupancy of the cation sites (now an average of 0·75 instead of 0·66) is described as varying periodically; the 'population wave' is normal to the (066) planes [$\equiv (066)_1$ for Sc_2S_3, although **b** and **c** are interchanged], and its value varies between 0·54 and 0·84 (Hariharan, Powell, Jacobson & Franzen, 1981).

The present paper describes the results of an electron microscope study of Sc_2S_3. High-resolution

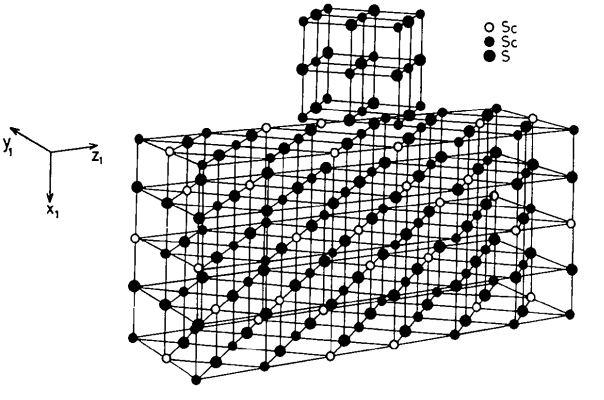

Fig. 1. A unit cell of the orthorhombic structure of Sc_2S_3 after Dismukes & White (1964). Large filled circles are S, small filled circles are Sc atoms, and small open circles are vacant cation sites (which would be occupied in ScS, but not in Sc_2S_3). At the top a unit cell of **NaCl**-type ScS is shown: it is a subcell of Sc_2S_3 structure.

* Present addresses: Departamento de Inorgánica, Facultad de Químicas, Universidad Complutense, Madrid-3, and Instituto de Química Inorgánica 'Elhuyar', CSIC, Madrid-6, Spain.

† Permanent address: Research Institute for Iron, Steel and Other Metals, Tohoku University, Sendai 980, Japan.

0108-7681/84/040355-05$01.50

structure images (which display the arrangement of vacant cation sites) and electron diffraction patterns will be discussed. Disorder and structure changes under the influence of electron-beam irradiation will also be considered.

Experimental methods

(*a*) *Sample preparation*

Scandium sesquisulphide was prepared by induction heating, in a stream of 5% H_2S + 95% Ar (10^5 Pa pressure; total flow rate ~0·05 $dm^3 s^{-1}$), of a carbon crucible containing Sc_2O_3 powder. The temperature was ~1773–1873 K, and the reaction time ~2 h. At the end of the preparation the sample was allowed to cool rapidly (in the gas stream) to room temperature. From this product single crystals were produced by chemical transport for 62 d, using I_2 as the transporting agent (1373 → 1273 K).

(*b*) *X-ray diffraction*

A Guinier–Hägg focusing camera (XDC-700) was used to obtain powder patterns. Monochromatic Cu $K\alpha_1$ radiation (λ = 1·5405981 Å) was employed, and 6N purity Si powder was used as an internal standard [a = 5·4305 (1) Å].

(*c*) *Electron microscopy/diffraction*

Crystals were ground under ethanol in an agate mortar, and dispersed on Cu grids coated with holey-carbon support films. These were examined in a JEOL 200 CX microscope fitted with an 'ultra-high-resolution' top-entry goniometer (±10°), an objective lens with C_s = 1·2 mm, and an LaB_6 filament. (Exposure times were ~2 s at a magnification of 550000×.)

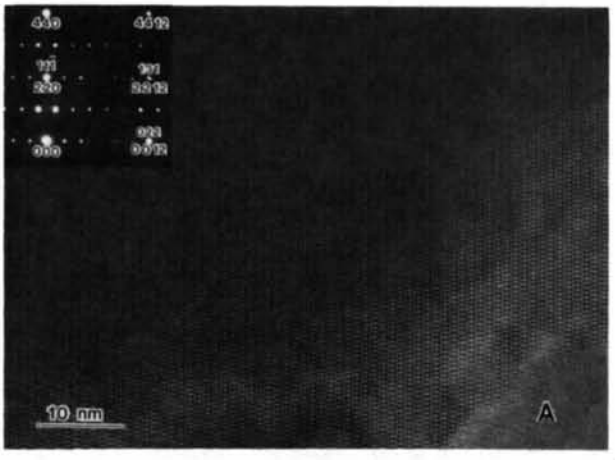

Fig. 2. Low-magnification electron-microscopy structure image of an Sc_2S_3 crystal. Inset at top left is the corresponding, indexed diffraction pattern: zone axis $[1\bar{1}0]_1$. The larger numbers (below a reflection) correspond to the Sc_2S_3 orthorhombic cell (1); the smaller numbers (above) correspond to the NaCl-type subcell.

Crystal fragments projecting over holes in the carbon film were tilted into the $[1\bar{1}0]_1 \equiv [2\bar{1}1]_0$ zone axis. Through-focal series of images were recorded using an objective aperture with $R = (1{\cdot}5\ \text{Å})^{-1}$. Transformation to disordered states was induced by focusing the beam, with the condenser aperture removed.

Observations and their interpretation

(*a*) *X-ray diffraction*

Unit-cell parameters, deduced from measurement of the Guinier films, were in good agreement with those of Dismukes & White (1964), above: a = 10·376 (2), b = 7·378 (1), c = 22·053 (3) Å for our original powder preparation, and a = 10·376 (2), b = 7·3775 (9), c = 22·033 (6) Å for the single-crystal preparation.

(*b*) *Electron microscopy*

Fig. 2 is a lower-magnification image and the corresponding electron diffraction pattern from the single-crystal preparation. The latter is indexed according to the orthorhombic cell (1) previously discussed, the most intense spots, such as $hk0$ and $hk12$ with h, k = $2n$, corresponding to the $B1$ subcell $\{(220)_1 \equiv (11\bar{1})_0$ and $(0,0,12)_1 \equiv (022)_0$; zone axis $[\bar{1}10]_1 \equiv [2\bar{1}1]_0\}$. The disappearance of normal contrast at the thin edge of the crystal (A) is characteristic of most metal sulphides that we have examined, even if they are (thermodynamically) very stable compounds – resistant to aerial oxidation at high temperature, for example. Interpretable image structure occurs inside this band. Fig. 3 is an enlargement of

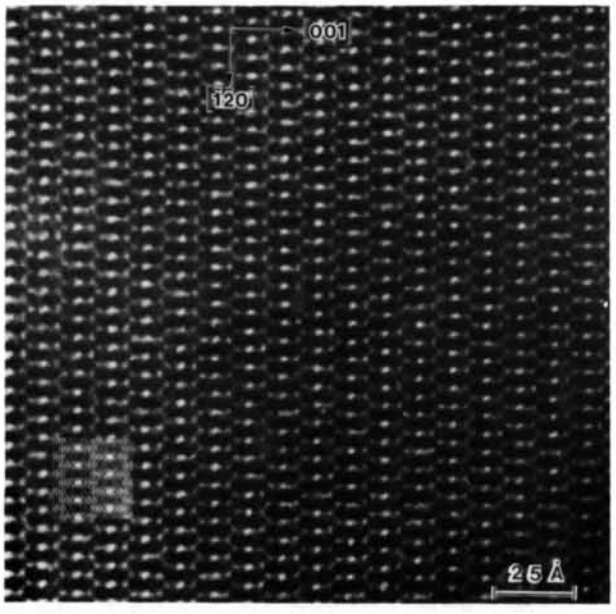

Fig. 3. A photographic enlargement of part of Fig. 2. Note the two types of white blobs arranged on an elongated hexagonal net. (Inset is a computed image; *cf.* Fig. 5.)

part of Fig. 2. The contrast consists of white blobs (stronger and weaker) arranged on an elongated hexagonal net; we shall show that they correspond to the vacant cation sites in the structure of Dismukes & White (1964).

The arrangement of these vacant sites is most easily seen if the structure is projected on to the $(\bar{2}10)_1 \equiv (\bar{2}1\bar{1})_0$ plane. Fig. 4 shows this projection of all the $B1$ cation sites (anions omitted). Each circle corresponds to two sites equally spaced along the projection axis, although they are at varying heights. In Sc_2S_3 the occupied sites correspond to the filled circles, the unoccupied sites to the open circles. Simulations of the experimental images (for this zone axis) were calculated for various values of defocus and crystal thickness by the multislice method (Cowley & Moodie, 1957) using the *SHRLI* suite of computer programs described in O'Keefe & Buseck (1979) and

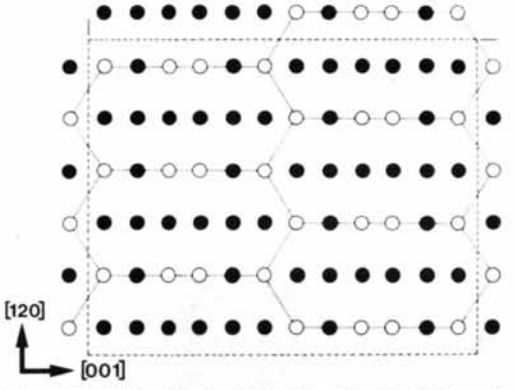

Fig. 4. A unit cell (outlined with broken lines) of the cations in the Sc_2S_3 structure projected along $[\bar{2}10]_1 = [\bar{2}1\bar{1}]_0$; zone axis = $[1\bar{1}0]_1 = [\bar{2}1\bar{1}]_0$. (S atoms are omitted.) In this projection two cations are superimposed along the translation repeat axis. Filled and open circles represent respectively fully occupied Sc sites and empty sites (which would be occupied in $B1$-type ScS).

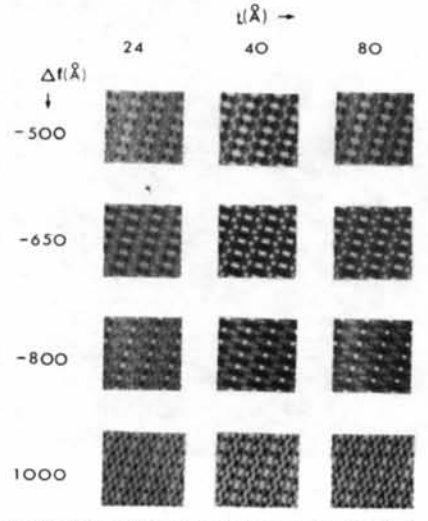

Fig. 5. A selection of computed images for Sc_2S_3 in projection along $[\bar{2}20]_1$ (zone axis $[1\bar{1}0]_1$) for various values of defocus, Δf, and crystal thickness, t.

appropriate parameters (thickness per slice Z = 1·595 Å, 500 beams, beam-convergence semi-angle = 0·80 mrad). The results are shown in Fig. 5. Clearly agreement is satisfactory for a defocus around Δf = −800 Å, and a thickness of ~40 Å. The brightest white blobs correspond to closely spaced (~1·88 Å) pairs of rows of 'vacant sites', and the less bright ones to isolated rows (distance ~3·53 and ~3·71 Å from nearest-neighbour vacancy rods, see Fig. 4).

(c) *Electron microscopy of disordered* Sc_2S_3

The image in Fig. 2 (and Fig. 3) suggests that the crystal structure is virtually perfect over the whole

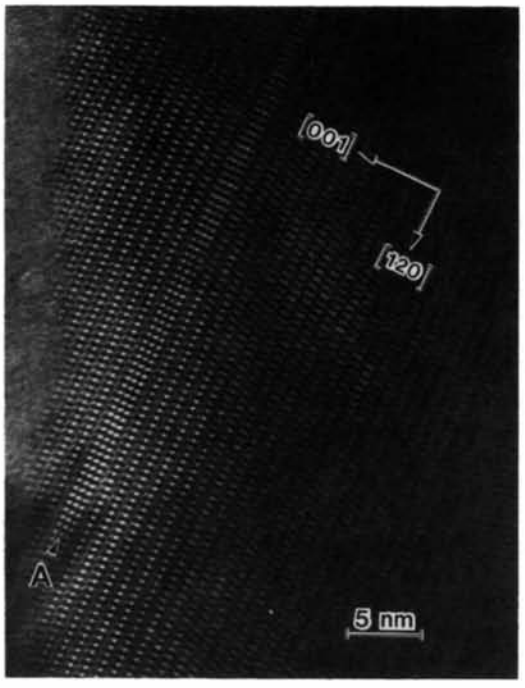

(a)

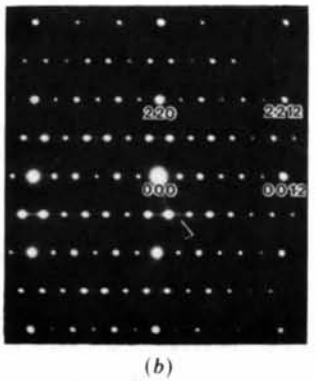

(b)

Fig. 6. (*a*) High-resolution image showing an extended defect *A*. Apart from the defect, the contrast is similar to that in Fig. 3. (*b*) $[1\bar{1}0]_1$ zone-axis diffraction pattern corresponding to (*a*): indices correspond to the orthorhombic *Fddd* unit cell. The forbidden reflections at 002, 006, ... and 222, 226 ... *etc.* appear by double diffraction. But note the slight streaking along $\mathbf{c}^*$, and a few very weak additional reflections, *e.g.* at $\bar{1}\bar{1}2$ (arrowed).

area; and many but not all crystals examined had a similar appearance. Some contained lamellar defects, as shown for example in Fig. 6(*a*). [The corresponding diffraction pattern is in Fig. 6(*b*).] We cannot be certain that these faults were *not* a result of irradiation by the electron beam, but we suspect that this is the case; *i.e.* that they are growth faults. Naive interpretation of the image contrast along the lines used above for the perfect crystal suggests that they are simple antiphase boundaries (APB's) produced by the formal mechanism shown in Fig. 7; the displacement vector projected on to the $(\bar{1}10)_1$ plane being $\mathbf{R} = \frac{1}{6}[110]_1$.

We have observed lamellar faults of this sort with various widths, all $n \times c/2$ [n an integer = 1 for the parent structure, 2 for fault A in Fig. 6(*a*), 3 . . . , *etc.* in other cases]. Some, no doubt, *are* produced by irradiation. And it is abundantly clear that decomposition of the sample in the electron beam starts preferentially at such faults; a good example is given in Fig. 8. Fig. 9 is an example of a crystal heavily decomposed by severe and prolonged (10–15 min) irradiation by the beam.

Fig. 10 is another example of a less-severely decomposed crystal. In the corresponding diffraction pattern the rows *hhl* with $h = 2n$ now contain only those reflections with $l = 4n$. The $l = 2n$ reflections previously present as a result of double diffraction [Figs. 2 and 6(*b*)] are now absent because (due to the disorder) the parent diffraction vector ($\Delta l = 2$ in *hhl* rows with $h = 2n + 1$) is no longer present. These rows are heavily streaked; they do *not* contain fundamental Bragg reflections characteristic of the $B1$ subcell; their reflections result from the superlattice, which is clearly being destroyed.

It appears likely that the changes are due to loss of S from the specimen; and it is relevant that

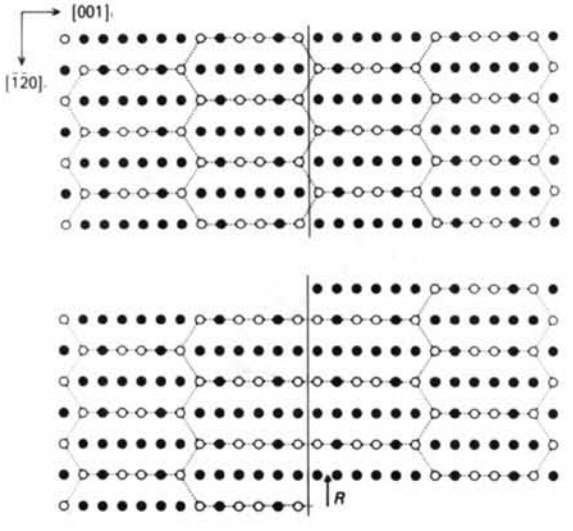

Fig. 7. Production of a planar fault by slip in Sc_2S_3. The structure in the fault region appears to be that of A in Fig. 6(*a*).

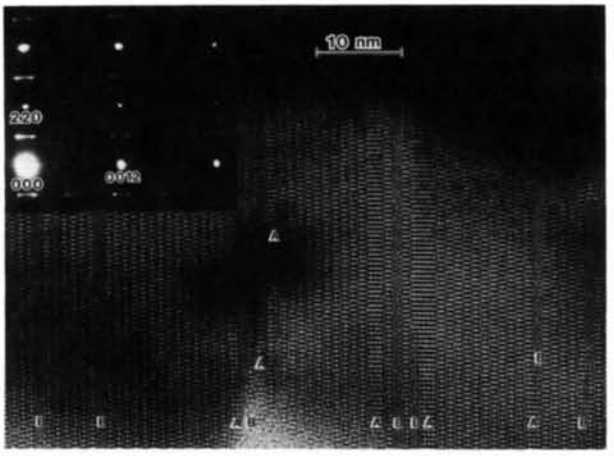

Fig. 8. High-resolution image after the specimen was irradiated with the electron beam. Inset (top left) is the corresponding diffraction pattern, zone axis $[1\bar{1}0]_1$. Apart from extended defects A, mainly of type similar to that in Fig. 6(*a*), there are other defects B, not yet identified. The latter occur preferentially around A, and appear to replace A. The diffraction pattern suggests extensive decomposition/disorder: the main Bragg reflections are for the $B1$ subcell (with slight streaking).

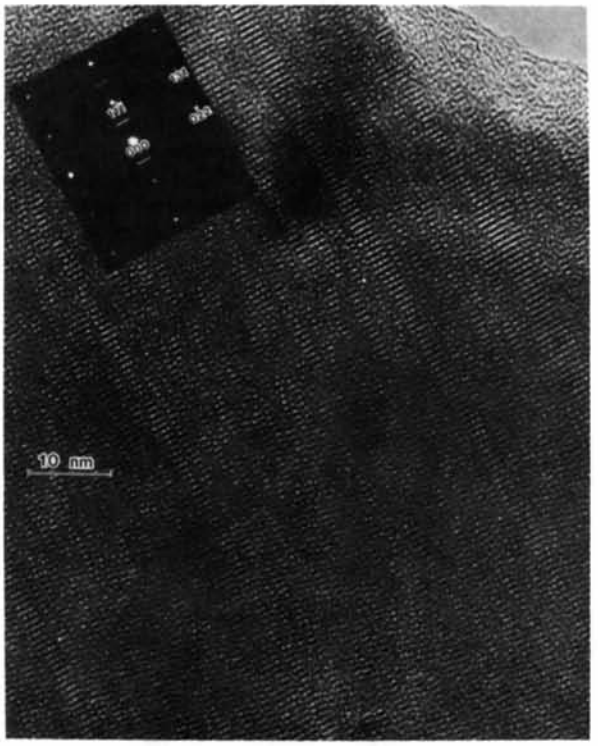

Fig. 9. Image similar to that in Fig. 8, but of a very heavily decomposed area of an Sc_2S_3 crystal. Inset (top left) is the corresponding diffraction pattern, indexed for the $B1$ subcell. It is similar to that in Fig. 8, except that the *Fddd* reflections have almost disappeared.

Dismukes & White (1964) have reported another superstructure with a $B1$ subcell for the stoichiometry $Sc_{1\cdot37}S_2 = ScS_{1\cdot46}$ (which is S-deficient with respect to Sc_2S_3). And there is also $B1$-type ScS of course: however, the image of the decomposed areas (B) does not correspond to ScS.

The decomposition has not yet been sufficiently studied to determine what the eventual product(s) might be. But it is clear that all these three structures are rather similar, topologically and metrically, so that coherent domains of at least two of them (in a 'non-stoichiometric crystal') are a quite plausible decomposition path. (Notice the parallel evolution of diffraction patterns with images during decomposition. Their appearance suggests a transformation towards $B1$-type ScS.)

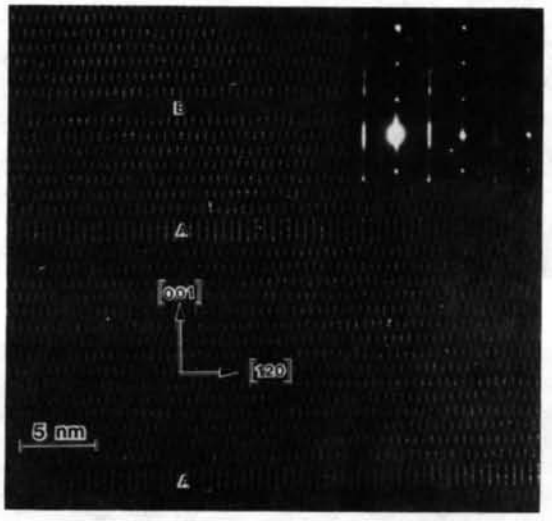

Fig. 10. Image of a partly decomposed crystal showing A and B lamellae (*cf.* Fig. 8). 1·8 Å (0,0,12) fringes are visible in the original print. Inset: corresponding diffraction pattern; zone axis $[1\bar{1}0]_I$. The disorder in the *Fddd* superlattice [parallel to (001)] has destroyed the Bragg reflections in rows hkl with $h = 2n+1$. Those in the rows with $h = 2n$ correspond to the *Fddd* cell with correct extinctions. (Double diffraction from the other rows is absent.)

We are grateful to Mr Peter Barlow for assisting with the electron microscopy. One of us (LCO-D) wishes to thank the Research School of Chemistry for a Visiting Fellowship which enabled this work to be completed.

References

COWLEY, J. M. & MOODIE, A. F. (1957) *Acta Cryst.* **10**, 609–619.
DISMUKES, J. P. & WHITE, J. G. (1964). *Inorg. Chem.* **3**, 1220–1228.
DISMUKES, J. P. & WHITE, J. G. (1965). *Inorg. Chem.* **4**, 970–973.
FLAHAUT, J. (1979). *Handbook of the Physics and Chemistry of Rare Earths.* Vol. 4. *Non-metallic Compounds.* II, edited by K. A. GSCHNEIDER & L. EYRING, pp. 1–89. Amsterdam: North-Holland.
FLAHAUT, J. & LARUELLE, P. (1968). *Prog. Sci. Technol. Rare Earths*, **3**, 151–208.
HARIHARAN, A. U., POWELL, D. R., JACOBSON, R. A. & FRANZEN, H. F. (1981). *J. Solid State Chem.* **36**, 148–150.
KLEMM, W., MEISEL, K. & VON VOGEL, H. U. (1930). *Z. Anorg. Allg. Chem.* **190**, 123.
MEN'KOV, A. A., KOMISATOVA, L. N., SIMANOV, YU. P. & SPITSYN, V. I. (1961*a*) *Dokl. Akad. Nauk SSSR*, **141**, 364–367.
MEN'KOV, A. A., KOMISATOVA, L. N., SIMANOV, YU. P. & SPITSYN, V. I. (1961*b*). *Dokl. Chem. (Engl. Transl.)* **141**, 1137–1140.
MEN'KOV, A. A., KOMISATOVA, L. N., SIMANOV, YU. P. & SPITSYN, V. I. (1962). *Chem. Abstr.* **56**, 9543*a*.
O'KEEFE, M. A. & BUSECK, P. R. (1979). *Trans. Am. Crystallogr. Assoc.* **15**, 27–46.
PICON, M., DOMANGE, L., FLAHAUT, J., GUITARD, M. & PATRIE, M. (1960). *Bull Soc. Chim. Fr.* pp. 221–228.
ROOYMANS, C. J. M. (1959). *J. Inorg. Nucl. Chem.* **11**, 78.

Acta Cryst. (1984). B**40**, 359–363

RHEED-Untersuchungen einer Grenzschichtstruktur von SnO_2 auf Quarz

VON EBERHARD MÜLLER

Sektion Chemie der Friedrich-Schiller-Universität Jena, DDR-6900 Jena, Deutsche Demokratische Republik

(*Eingegangen am* 28. *Februar* 1983; *angenommen am* 5. *März* 1984)

Abstract

An unknown epitaxial interface phase of SnO_2 on α-quartz(10$\bar{1}$0) was investigated by RHEED. SnO_2II crystallizes in the space group *Pbcn*. Octahedra sharing a common edge form zigzag chains in the case of SnO_2II, unlike SnO_2 which has the rutile structure. Thus in the resulting intergrowth structure all the surface O atoms of quartz may be used to build up the octahedra of SnO_2II.

Einleitung

Bei reaktiver Abscheidung aus der Gasphase und Temperung bei 850 K ist ein epitaktisches Verwachsen von SnO_2 auf α-Quarz(10$\bar{1}$0) möglich, wobei als Verwachsungsebene die ungewöhnlich hoch indizierte Ebene (11,0,5) auftritt (Bräuer, Meyer, Müller & Müller, 1981). Mit den Gitterparametern des SnO_2 (Baur, 1956) und des α-Quarzes (*Landolt–Börnstein*, 1975) ergeben sich relative Fehlpassungen

0108-7681/84/040359-05$01.50